

# Functional Film with Electric-Field-Aided Aligned Assembly of Quantum Rods for Potential Application in Liquid Crystal Display

Sandeep Kaur, G. Murali, Ramesh Manda, Young Cheol Chae, Minhee Yun, Joong Hee Lee, and Seung Hee Lee\*

**Harnessing the unique polarized light emission characteristic from semiconductor quantum rods (QRs) necessitates their large-area unidirectional alignment. Herein, the aligned assembly of CdSe/CdS QRs is demonstrated by fabricating a functional film on a micrometer-spaced interdigitated electrodes substrate over an area of  $\approx 1.3$  cm<sup>2</sup>. The external electric field is used to control the position and orientation of QRs which is later frozen by the polymerization of reactive mesogen under the exposure of UV light. Under the fluorescence microscope, a judicious change in the QRs emission intensity with the polarizer axis positioned parallel and perpendicular to the alignment direction suggests the optical anisotropy. The degree of alignment of QRs is characterized by the polarization ratio which is measured 0.48 from the photoluminescence spectra. It is found that factors such as optimal QRs concentration and the presence of liquid crystal contributed for better QRs alignment. Such films may be advantageous for liquid crystal display devices to accomplish light polarization and wider color gamut.**

With the discovery of an intermediate state of matter between isotropic liquid and crystalline solid about a century ago and subsequently their use in display application in the late 1970s, the liquid crystal display (LCD) technology is persistently evolving with the development of new materials and technologies. Nowadays, owing to the diversity in the size of display devices, e.g., large-screen TVs, computers, tablets, smart phones, and smart watches, different display modules prevail and vie for their market share. The LCD technology has

conquered the large-area display market owing to its advantages such as higher resolution and longer lifetime, but faced challenges from OLED devices in terms of module thickness, response time, and vivid colors.<sup>[1]</sup> The traditional LCD technology uses blue light-emitting diodes (LEDs) coupled with a yellow phosphor to originate a white light which is transmitted through an assembly of devices comprising polarizers, thin-film transistor array, liquid crystals, and color filters.<sup>[2]</sup> However, the wide transmission through the color filters and broad emission spectrum of yellow phosphor practically inhibits the realization of wider color gamut in such LCD devices.<sup>[3]</sup>

Semiconductor quantum rods (QRs), owing to their higher brightness,<sup>[4]</sup> color purity,<sup>[5]</sup> and polarized light emission<sup>[6]</sup> features, are lending prominent prospects

for their application in display technology. The use of quantum dots in the backlight unit in the form of quantum-dot enhancement film has already been demonstrated<sup>[7]</sup>; however, the emission from these spherical particles is isotropic. A unidirectional aligned array of QRs coupled with LCD backlight can be foreseen as a viable option to attain wider color gamut and light polarization.<sup>[8]</sup> A polarized blue light coming from either laminated conventional polarizer or in-cell coated polarizer can stimulate the QRs to provide narrow red and green polarized emission (**Figure 1**). This can result in reduced color crosstalk, and hence LCD with high color gamut and contrast ratio can be realized.

The alignment of QRs is crucial to attain maximum polarized light emission. Several approaches have been demonstrated in the past on this pathway such as by utilizing photoalignment technology,<sup>[9]</sup> mechanical rubbing,<sup>[10]</sup> assembly in liquid crystal defects,<sup>[11]</sup> and solvent evaporation-assisted assembly.<sup>[12]</sup> Furthermore, QRs embedded in nanofibers sheets using electrospinning<sup>[13]</sup> and mechanical stretching of polymer film<sup>[14]</sup> have been reported with higher degree of alignment. The use of external electric field has been well known to arrange QRs as both parallel<sup>[15,16]</sup> and perpendicular<sup>[17]</sup> to the substrate. Herein, we report a simplistic approach for unidirectional alignment of CdSe/CdS QRs by utilizing external electric field after mixing in solvent-based reactive mesogen (RM). The QRs showed higher

S. Kaur, Dr. G. Murali, R. Manda, Y. C. Chae,  
Prof. J. H. Lee, Prof. S. H. Lee  
Department of BIN Convergence Technology  
Chonbuk National University  
Jeonju 54896, South Korea  
E-mail: lsh1@chonbuk.ac.kr

Prof. M. Yun  
Department of Electrical and Computer Engineering  
Swanson School of Engineering  
University of Pittsburgh  
Pittsburgh, PA 15261, USA

Prof. S. H. Lee  
Department of Polymer Nano-Science and Technology  
Chonbuk National University  
Jeonju 54896, South Korea

DOI: 10.1002/adom.201800235

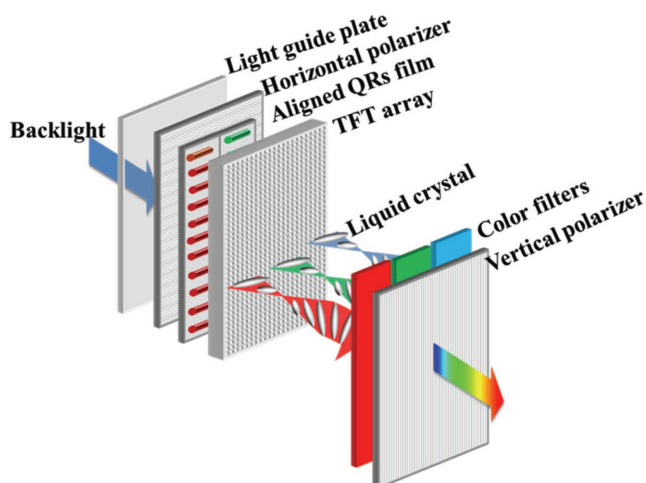


**Figure 1.** Schematic illustration. A unidirectional aligned functional film of red and green emissive QRs embedded in LCD architecture.

degree of alignment in the proximity of RM molecules and the polarization ratio ( $\rho$ ) from aligned QRs array was calculated from photoluminescence (PL) spectra as  $\rho = (I_{\parallel} - I_{\perp}) / (I_{\parallel} + I_{\perp})$ , where  $I_{\parallel}$  and  $I_{\perp}$  represent the respective PL intensities, parallel and perpendicular to the field direction. The fluorescence (FL) microscope images of the sample with the polarizer gave the evidence of polarization anisotropy of QRs and the alignment of RM was confirmed under polarizing optical microscope (POM).

The ligand (methoxy polyethylene glycol (mPEG)) coated red emissive CdSe/CdS QRs showed absorption peak at 430 nm, and PL emission peak was measured at 626 nm with the excitation wavelength of 405 nm. The value of full width at half maximum was calculated as 26 nm (Figure 2a). The transmission electron microscope (TEM) images revealed the average length and diameter of QRs about 46 and 5 nm, respectively (Figure 2b). A commercially available RM, RMS-03-013C was used for this work in which RM having positive dielectric anisotropy ( $\Delta n = 0.137$  at 589 nm (data sheet supplied by Merck))

is dissolved in propylene glycol monomethyl ether acetate (PGMEA) solution. The steps followed for the formation of QRs film are illustrated in Figure 2c. In the absence of applied field, the RM molecules showed random orientation under POM. No visible large-sized aggregates were found under microscope after coating the RM/QRs mixture on the in-plane switching (IPS) substrate (Figure S1, Supporting Information). We expect that the slight presence of PGMEA in the RM/QRs mixture prevents the formation of hefty bundles of QRs. The PGMEA was evaporated slowly by gradually increasing the applied field. As the voltage was increased from 0 V, the RM molecules started gradually orienting along the applied field direction, and the disclination lines started to disappear (Figure S1, Supporting Information). Under the applied field, RM molecules were driven by external bias to minimize the electrostatic energy of the system, and their LC director aligns parallel to the field direction. At 80 V, the entire electrode area showed uniform homogeneous alignment of RM and the field within the gap area was estimated as  $26.6 \text{ V } \mu\text{m}^{-1}$  from the relation  $E = V/l$ , where  $V$  is the voltage at which RM molecules showed uniform alignment and  $l$  is the gap between the electrodes. The anchoring force between QRs and LC present in RM provides large alignment energy, which is expected to drive QRs along the RM molecule direction.<sup>[18]</sup> Additionally, QRs acquire large permanent dipole moment along the wurtzite  $c$ -axis due to their noncentro-symmetric lattice structure. Besides, the large dielectric constant of QRs results in induced dipole moment, which is proportional to the magnitude of the applied electric field. As the QRs are subjected to the applied field, it produces electric field induced torque resulting in their orientation along the field lines while evaporating the solvent and confining them in a unidirectional array.<sup>[16]</sup>

After getting uniform alignment of RM, the complete dark and bright states were realized under the crossed polarizers, with electrodes direction positioned at an angle of  $0^\circ$  and  $45^\circ$  along with one of the polarizer (Figure 3a). Thereafter, the orientation of the RM molecules and QRs was frozen after irradiating with the UV light. The field was removed after polymerization, and dark and bright states remained intact

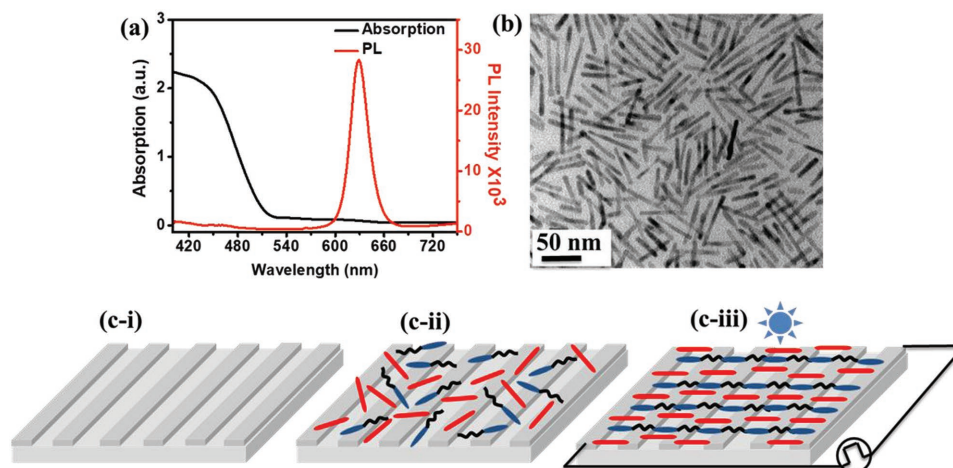


**Figure 2.** a) Absorption and PL emission spectra of CdSe/CdS QRs and b) corresponding TEM image. Pictorial depiction of method followed to prepare QRs functional film: c-i) IPS substrate, c-ii) RM/QR mixture after coating on IPS substrate, c-iii) RM/QR mixture on IPS substrate under applied in-plane ac square field and illuminated with UV light.

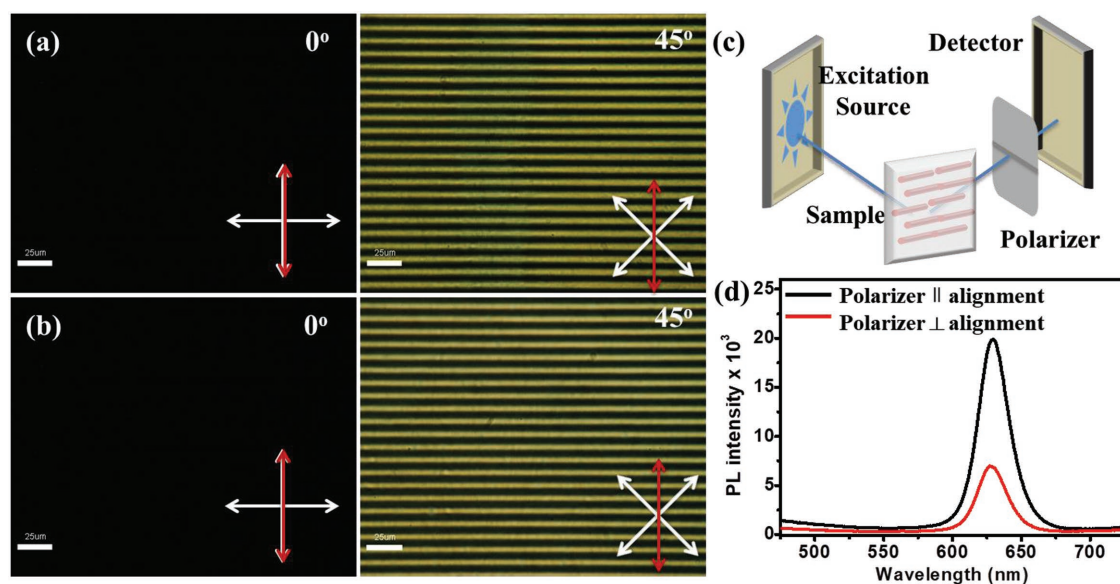


**Figure 3.** POM images of RM/QRs mixture taken on IPS substrate by changing the polarizer angle a) under applied field and before UV curing, b) UV cured film after removing the field (scale – 25 μm). c) Experimental setup to measure PL spectra by inserting a polarizer and d) PL spectra measured from functional film on IPS substrate.

(Figure 3b). Polarization-dependent PL emission spectra of the film were measured by placing the polarizer parallel and perpendicular to the orientation of RM molecules (Figure 3c). When the polarizer axis was positioned parallel to the alignment direction, the PL intensity was measured higher than in the perpendicular position. The polarization ratio value was calculated as 0.48 from the PL spectra (Figure 3d). The reduced PL intensity along the perpendicular position is mainly due to the alignment of QRs along the field direction.

To further confirm the QRs alignment, the film was analyzed under FL microscope with polarizer positioned parallel and perpendicular to the alignment direction. The emission intensity from QRs was found to be higher when polarizer axis was parallel to alignment direction (Figure 4a) and was decreased when the polarizer was rotated by 90° (Figure 4b), which confirmed polarization anisotropy of QRs. Few bright spots were observed (marked with arrows), which represent tiny QRs aggregates. The FL intensity of such bright spots remains almost unaltered either with the polarizer being placed parallel or perpendicular to the alignment direction. This indicates that the QRs within these aggregates are not well aligned, which can be attributed

to the lower polarization ratio. Except few aggregates, the rest of the entire area of the film showed uniform polarization anisotropy. The thickness of homogeneously aligned cured RM film was estimated from the retardation plot as 0.9 μm ( $d\Delta n = 0.129 \mu\text{m}$ ) at 589 nm. The polarization-angle-dependent PL spectra of the film are presented in Figure 4c. The black fitted curve showed  $\cos^2\theta$  dependence of PL emission intensity with varying polarizer angle, which is quite in agreement with the Malus' law ( $I(\theta) = I_0 \cos^2\theta$ ).

To get the insight about QRs directional arrangement, the film was observed under field emission-scanning electron microscope (FE-SEM). The film analyzed from the top of the ITO substrate did not provide any substantial information, as it was difficult to locate QRs in the polymer network (Figure S2a, Supporting Information). To get more clear impression, the film was pasted on the carbon tape with upside down and then examined under FE-SEM. The upturned images revealed QRs embedded in narrow-lined patterned arrangement (Figure S2b, Supporting Information). The majority of QRs were found to accumulate in the electrode gap and along the electrode edges (Figure S2c, Supporting Information), while few QRs were also

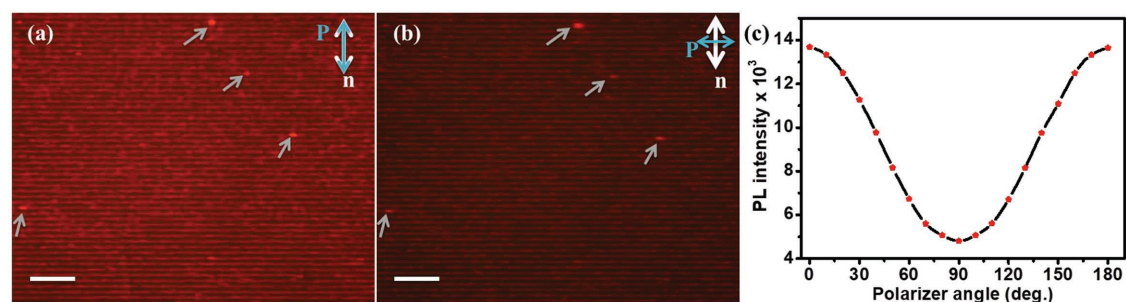


**Figure 4.** FL microscope images of the film with polarizer positioned a) parallel and b) perpendicular to the alignment direction (scale 100 μm). The arrows marked represent the small QRs aggregates. c) PL intensity variation of the film with varying polarizer angle.



seen over the top of the electrode area (Figure S2d, Supporting Information). Owing to uneven electric field distribution in the IPS substrate (Figure S2e, Supporting Information), the LC director in RM tends to align with a small inclination near to the electrode edges, and consequently, the QRs accumulated in this area are slightly tilted. However, as the film thickness is lesser than the gap length, the QRs experienced rather uniform in-plane field at the center of the electrode gap area and thus resulted in a unidirectional in-plane arrangement. The uneven arrangements of QRs found on the electrode top area are due to the irregular field distribution and inferior in-plane anchoring energy owing to the azimuthal orientation of LC director. As a result, the QRs emission from the top of the electrode area is rather unpolarized, therefore, decreasing the polarization ratio of the film. We expect that IPS substrate with even lower electrode width can reduce the nonuniform electric field region, and hence polarization ratio value may improve. Moreover, an IPS cell fabricated in an alternative way can be used to get improved polarized light emission. In this approach, first, the mixture should be coated on the glass substrate, bringing the IPS substrate over its top.<sup>[19]</sup> Thereafter, by slowing moving the top IPS substrate under the applied field, nonuniform field regions can be minimized, and they may give even more regular arrangement of QRs with improved polarization ratio.

From the FE-SEM images, it is clear that the film withstands under the high electric field even after being peeled off from the IPS substrate (Figure S3, Supporting Information). The fabricated film upheld the same polarization ratio value for longer period of time after being removed from the IPS substrate. The optical density of QRs in the film was measured as 1.2 at 460 nm. The QRs used in this study showed PL quantum yield of 70% which is lower than the ones in some recently published reports.<sup>[5,20]</sup> Such films fabricated with QRs having much higher PL quantum yield and increased polarization ratio are expected to enhance the optical efficiency of the LCD device up to 7%.<sup>[10]</sup> The high-resolution confocal microscope images recorded the maximum PL emission intensity near the electrode edges and gap region, owing to the presence of large number of QRs in this area (Figure S4, Supporting Information).

We have performed additional experiment with higher QRs concentration in RM solution. With increasing the concentration of QRs in RM solution to 1 wt%, the polarization ratio was decreased from 0.48 to 0.37. The POM images of the sample did not show any significant change (Figure S5, Supporting Information), as the dark and bright states of RM appeared same as in the previous case. However, the FL microscope with polarizer (Figure S5, Supporting Information) and confocal images (Figure S6, Supporting Information) revealed a densely packed network of QRs, and only a limited change in emission intensity was observed by changing the polarizer position parallel or perpendicular to the field direction (Figure S5, Supporting Information). As the number of QRs aligned by LC molecules is limited,<sup>[21]</sup> the optimum concentration of QRs in RM is crucial to achieve higher polarization ratio. Additionally, we have analyzed the sample in the absence of electric field. The RM/QRs mixture was coated uniformly on IPS substrate, and after completely evaporating the solvent from the mixture it was cured under UV light. The film did not show any dark and bright states under POM, as the RM was not well aligned

and polarization ratio from such sample was measured as 0.12. Such a low value was the result of randomly orientated QRs in the absence of electric field (Figure S7, Supporting Information).

Furthermore, to investigate the contribution from LC anchoring and applied field on QRs alignment, we prepared a QRs mixture in NOA63 with QRs concentration as 0.2 wt%. Thereafter, the mixture was coated on IPS substrate and was subjected to similar magnitude of electric field and subsequently polymerized under UV light. The polarization ratio calculated from this sample was 0.20, which was lower than that of QRs in RM sample (Figure S8, Supporting Information). This indicates that the LC molecules assist the QRs for better alignment as compared with other monomers.

In conclusion, here we present a facilitated approach to fabricate a unidirectional aligned QRs functional film by mixing them in RM solution. The solvent present in RM prevents the aggregation of QRs, and external electric field permits the QRs to orient along the field direction and guides their unidirectional assembly within the electrode gap of IPS substrate. The polarization ratio of the functional film obtained with applied field has found to be much higher than that obtained with the use of monomer. Such films are worthwhile for polarizers and patterned color filter array. Due to the simplicity and cost effectiveness, our approach enables to advance the LCD device structures by enhancing the optical efficiency and wider color gamut of the device.

## Experimental Section

**RM/QRs Mixture:** A colloidal dispersion of QRs (CAN GmbH-Hamburg, Germany) was prepared by adding 5 mg of QRs in 500  $\mu\text{L}$  of toluene by ultrasonication for few minutes. Thereafter, two different solutions of RM/QRs mixture were prepared by adding 20 and 100  $\mu\text{L}$  of QRs solution in 100 mg of RMS-03-013C to maintain the QRs concentration as 0.2 and 1 wt%, respectively. The RM/QRs solutions were then subjected to vigorous stirring for 36 h at 40  $^{\circ}\text{C}$  to slowly evaporate toluene. The optimal QRs concentration of 0.2 wt% was used for fabrication of the film.

**Fabrication of Functional Film:** The IPS substrate having interdigitated patterned ITO electrodes with width and gap of 4 and 3  $\mu\text{m}$ , respectively, was used for the experiment. The substrates were cleaned by means of ultrasonication in acetone and subsequently in distilled water for 5 min each, and were then dried at 80  $^{\circ}\text{C}$  in oven for almost 15–20 min. Thereafter, the RM/QRs mixture was dropped on IPS substrate and was spin coated at 1500 rpm for 15 s. After coating the mixture, the substrate was immediately subjected to an in-plane ac square field at frequency 1 kHz, and the voltage was gradually increased from 0 V. The RM orientation was monitored under POM with crossed polarizer and at 80 V the whole substrate showed uniform alignment of RM. Once the RM molecules showed homogeneous alignment under POM, the sample was irradiated with UV light having intensity 25  $\text{mW cm}^{-2}$  for 2 min under the applied field. After polymerization, the field was removed and sample was analyzed again under POM.

**Characterization:** Optical images were taken with POM (Nikon eclipse E600 POL) with a CCD camera (Nikon, DXM 1200). UV-visible spectra were acquired with a UV-visible spectrophotometer (SINCO, South Korea). TEM samples were analyzed with a TEM (Hitachi). The PL spectra were measured by Spectrofluorophotometer (Shimadzu). Inverted confocal microscope (Carl Zeiss) was used to take fluorescent images of QRs. The FE-SEM images of the film were taken after thin platinum coating with JEOL JSM-5900/Hitachi from Tokyo, Japan.

## Supporting Information

Supporting Information is available from the Wiley Online Library or from the author.

## Acknowledgements

This research was supported by the Basic Science Laboratory Research Program (2014R1A4A1008140) through the National Research Foundation of Korea (NRF) funded by the Ministry of Science, ICT & Future Planning.

## Conflict of Interest

The authors declare no conflict of interest.

## Keywords

photoluminescence, polarization ratio, polarized light emission, quantum rods, reactive mesogen

Received: February 21, 2018

Revised: April 28, 2018

Published online: June 25, 2018

- 
- [1] Z. Luo, D. Xu, S. T. Wu, *J. Display Technol.* **2014**, *10*, 526.  
 [2] K.-H. Kim, J.-K. Song, *NPG Asia Mater.* **2009**, *1*, 29.  
 [3] a) H.-W. Chen, R.-D. Zhu, J. He, W. Duan, W. Hu, Y.-Q. Lu, M.-C. Li, S.-L. Lee, Y.-J. Dong, S.-T. Wu, *Light Sci. Appl.* **2017**, *6*, e17043;  
 b) H. Chen, J. He, S. T. Wu, *IEEE J. Sel. Top. Quantum Electron.* **2017**, *23*, 1.  
 [4] D. V. Talapin, R. Koeppel, S. Götzinger, A. Kornowski, J. M. Lupton, A. L. Rogach, O. Benson, J. Feldmann, H. Weller, *Nano Lett.* **2003**, *3*, 1677.  
 [5] I. Coropceanu, A. Rossinelli, J. R. Caram, F. S. Freyria, M. G. Bawendi, *ACS Nano* **2016**, *10*, 3295.

- [6] a) J. Hu, L.-s. Li, W. Yang, L. Manna, L.-w. Wang, A. P. Alivisatos, *Science* **2001**, *292*, 2060; b) R. A. Hikmet, P. T. Chin, D. V. Talapin, H. Weller, *Adv. Mater.* **2005**, *17*, 1436.  
 [7] a) E. Jang, S. Jun, H. Jang, J. Lim, B. Kim, Y. Kim, *Adv. Mater.* **2010**, *22*, 3076; b) J. Chen, V. Hardev, J. Yurek, *Nanotechnol. Law Business* **2014**, *11*, 4.  
 [8] Z. Luo, Y. Chen, S.-T. Wu, *Opt. Express* **2013**, *21*, 26269.  
 [9] a) T. Du, J. Schneider, A. K. Srivastava, A. S. Susha, V. G. Chigrinov, H. S. Kwok, A. L. Rogach, *ACS Nano* **2015**, *9*, 11049; b) J. Schneider, W. Zhang, A. K. Srivastava, V. G. Chigrinov, H.-S. Kwok, A. L. Rogach, *Nano Lett.* **2017**, *17*, 3133.  
 [10] A. K. Srivastava, W. Zhang, J. Schneider, A. L. Rogach, V. G. Chigrinov, H. S. Kwok, *Adv. Mater.* **2017**, *29*, 1701091.  
 [11] a) Y. Amit, A. Faust, I. Lieberman, L. Yedidya, U. Banin, *Phys. Status Solidi A* **2012**, *209*, 235; b) L. Hartmann, D. Djurado, I. Florea, J.-F. Legrand, A. Fiore, P. Reiss, S. Doyle, A. Vorobiev, S. p. Pouget, F. d. r. Chandezon, *Macromolecules* **2013**, *46*, 6177; c) J. Kim, J. Peretti, K. Lahlil, J. P. Boilot, T. Gacoin, *Adv. Mater.* **2013**, *25*, 3295.  
 [12] L. Pelliser, M. Manceau, C. Lethiec, D. Coursault, S. Vezzoli, G. Leménager, L. Coolen, M. DeVittorio, F. Pisanello, L. Carbone, *Adv. Funct. Mater.* **2015**, *25*, 1719.  
 [13] a) A. Rizzo, C. Nobile, M. Mazzeo, M. D. Giorgi, A. Fiore, L. Carbone, R. Cingolani, L. Manna, G. Gigli, *ACS Nano* **2009**, *3*, 1506; b) A. M. Hung, N. A. Konopliv, J. N. Cha, *Langmuir* **2011**, *27*, 12322.  
 [14] a) M. Hasegawa, Y. Hirayama, S. Dertinger, *Appl. Phys. Lett.* **2015**, *106*, 051103; b) T. Aubert, L. Palangetic, M. Mohammadimasoudi, K. Neyts, J. Beeckman, C. Clasen, Z. Hens, *ACS Photonics* **2015**, *2*, 583.  
 [15] P. D. Cunningham, J. B. Souza Jr., I. Fedin, C. She, B. Lee, D. V. Talapin, *ACS Nano* **2016**, *10*, 5769.  
 [16] Z. Hu, M. D. Fischbein, C. Querner, M. Drndić, *Nano Lett.* **2006**, *6*, 2585.  
 [17] M. Mohammadimasoudi, L. Penninck, T. Aubert, R. Gomes, Z. Hens, F. Strubbe, K. Neyts, *Opt. Mater. Express* **2013**, *3*, 2045.  
 [18] a) K. M. Ryan, A. Mastroianni, K. A. Stancil, H. Liu, A. Alivisatos, *Nano Lett.* **2006**, *6*, 1479; b) A. Singh, N. J. English, K. M. Ryan, *J. Phys. Chem. B* **2013**, *117*, 1608.  
 [19] J.-H. Lee, I. H. Jeong, J. H. Yu, K. H. Song, K.-U. Jeong, S.-W. Kang, M.-H. Lee, S. H. Lee, *Opt. Express* **2014**, *22*, 15315.  
 [20] I. Hadar, J. P. Philbin, Y. E. Panfil, S. Neyshtadt, I. Lieberman, H. Eshet, S. Lazar, E. Rabani, U. Banin, *Nano Lett.* **2017**, *17*, 2524.  
 [21] K.-J. Wu, K.-C. Chu, C.-Y. Chao, Y.-F. Chen, C.-W. Lai, C.-C. Kang, C.-Y. Chen, P.-T. Chou, *Nano Lett.* **2007**, *7*, 1908.